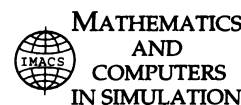




ELSEVIER

Mathematics and Computers in Simulation 55 (2001) 341–350



www.elsevier.nl/locate/matcom

Knot types, Floquet spectra, and finite-gap solutions of the vortex filament equation

Annalisa M. Calini*, Thomas A. Ivey

^a *Department of Mathematics, College of Charleston, Charleston, SC 29424, USA*

Received 1 October 2000; accepted 31 October 2000

Abstract

Using the connection between closed solution curves of the vortex filament equation and the periodic problem for the nonlinear Schrödinger equation (NLS), we investigate the possibility of relating the knot types of finite-gap solution to the Floquet spectra of the corresponding NLS potentials, in the special case of small amplitude curves close to multiply-covered circles. © 2001 IMACS. Published by Elsevier Science B.V. All rights reserved.

Keywords: Vortex filament equation; Nonlinear Schrödinger equation (NLS); Floquet spectra

1. Introduction

There are by now many examples of curve evolution described by soliton equations; it suffices to mention the vortex filament equation, also known as the localized induction equation (LIE), for vortex filament dynamics [9,12,13]; the mKdV equation modeling the motion of vortex patch boundaries [10] (as well as edges of planar electron droplets in a magnetic field [18]); the Sine–Gordon equation (SG) for constant torsion curves generating pseudospherical surfaces [4,5]; and their higher dimensional generalizations [8,14].

For equations, such as the LIE which correspond to curve dynamics in three-dimensional space, periodic boundary conditions have an additional implication: the corresponding curves can be closed (closure is preserved by the purely local flow) and may be knotted. On the other hand, the periodic theory of finite-gap solutions (periodic and quasi-periodic analogues of multi-solitons) is fairly well understood; recently, Grinevich and Schmidt [11] gave a precise characterization of the closure conditions for solutions of the LIE associated with periodic finite-gap potentials of the NLS equation.

In this article, we begin to investigate a possible relationship between the knot types of closed LIE solutions coming from finite-gap NLS potentials and (part of) their associated Floquet spectra. Finite-gap solutions of the LIE, as opposed to more general solutions, are good candidates for representing a large

* Corresponding author.

E-mail addresses: calinia@cofc.edu (A.M. Calini), iveyt@cofc.edu (T.A. Ivey).

class of knot representatives since, at least for a low number of phases, their topology appears to be preserved by the time evolution. Because of this, and because the time-dependence for these is through a linear phase, we can just study their knot types at a fixed time. Ultimately, our hope is to find canonical knot representatives among the solutions of integrable curve evolutions, with which to approximate generic knots (just as one can use finite-gap solutions to approximate generic periodic NLS initial data), and to investigate whether we can extract knot invariants for the restricted class of finite-gap curves from the hierarchy of conserved quantities encoded in the Floquet discriminant (see also [16]).

The connection between the LIE and NLS was discovered by Hasimoto [12]. If $\gamma(x, t)$ is an arclength parametrized position vector evolving by the LIE

$$\gamma_t = \gamma_x \times \gamma_{xx}, \quad (1)$$

with curvature κ and torsion τ then $q(x, t) = \kappa(x, t) \exp \left[i \int^x \tau(s, t) ds \right]$ satisfies the NLS equation

$$iq_t + q_{xx} + 2|q|^2 q = 0. \quad (2)$$

On the other hand, a technique due to Sym and Pohlmeier (described below in Section 2) allows one to reconstruct $\gamma(x, t)$ in terms of a fundamental matrix solution of the NLS Lax pair. For finite-gap potentials in the periodic and quasi-periodic cases, such matrices can be constructed from the Baker–Akheizer functions [2], which are defined in terms of theta functions on the Jacobian of a hyperelliptic Riemann surface whose branch points are the discrete part of the Floquet spectrum; moreover, such potentials may be characterized in terms of their periodic spectra.

The curves studied in this work are associated with periodic finite-gap NLS potentials close to modulationally unstable plane waves. Both their Floquet spectra and the expression for $\gamma(x, t)$ can be computed using perturbation techniques. Although a complete understanding of the relation between knot types and spectra of finite-gap curves requires the Baker function representation, the perturbation analysis done here yields several interesting results.

The spectrum of a modulationally unstable plane wave (see Fig. 1) contains a finite number of imaginary double points labeling its linear instabilities. It is well-known that the homoclinic manifold of an unstable

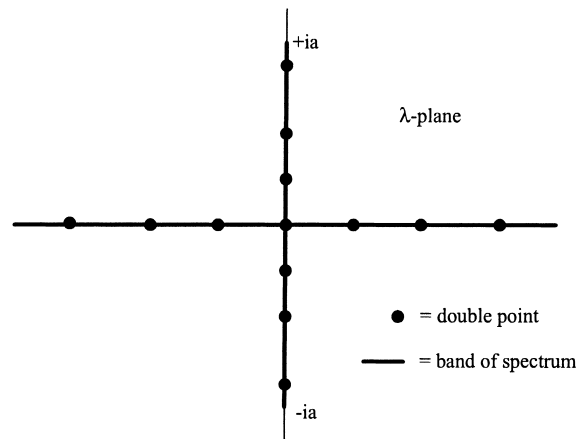


Fig. 1. The Floquet spectrum of a plane wave potential with three unstable modes. The corresponding curve is a triply covered circle.

NLS solution can be explicitly constructed using Bäcklund transformations. In previous work [3], the first author computed the LIE curves associated to homoclinic orbits of unstable plane waves: these curves are singular knots whose self-intersections persist throughout the time evolution. Since homoclinic orbits are degenerate finite-gap solutions (associated with singular Riemann surfaces), one can ask whether the corresponding singular knots separate curves of different knot types. We will give a positive answer to this question for a few low-genus cases.

In Section 2, we describe the Sym–Pohlmeyer reconstruction method and review some basic facts of Floquet theory, using a modulationally unstable plane wave as an example. We also review the conditions that the Floquet spectrum of a finite-gap curve must satisfy in order for the curve to be closed.

Section 3 describes the perturbation analysis, which builds on the work of Ablowitz et al. [1]. Although the curves produced by periodic perturbation of the plane wave potential are closed only to first order, Proposition 3.1 guarantees that quasiperiodic perturbations exist which produce, non-perturbatively, the same curves and spectra.

In Section 4 we describe the results of various experiments, both in the case of even perturbations which produce self-intersecting curves, and in the noneven case where genuine knots arise. For perturbations which split one of the complex double points, we formulate a precise conjecture on how its knot type relates to its Floquet spectrum.

2. The curve and the linear system

For a complex-valued potential $q(x)$, let $\psi(x)$ satisfy the spatial part of the Lax pair, also known as the Zakharov–Shabat spectral problem, for NLS:

$$\psi_x = \begin{pmatrix} i\lambda & q(x) \\ -\bar{q}(x) & -i\lambda \end{pmatrix} \psi. \quad (3)$$

(The complex eigenfunction $\psi(x)$ is vector-valued.)

For real values of the spectral parameter λ , (3) can be interpreted, as follows, as the Frenet–Serret equations for a curve in three-dimensional space with curvature $\kappa(x) = |q(x)|$ and torsion $\tau(x) = (d/dx) \arg[q(x)] - 2\lambda$. For $\lambda = 0$, this is the inverse of the Hasimoto map. The position vector of the curve is given in terms of the fundamental solution matrix $\Psi(x; \lambda)$ of (3) by the Sym–Pohlmeyer formula [15,17]:

$$\gamma(x) = \Psi^{-1}(x; \lambda_0) \left. \frac{d}{d\lambda} \Psi(x; \lambda) \right|_{\lambda=\lambda_0}, \quad \lambda_0 \in \mathbb{R}. \quad (4)$$

(We fix an isometry between \mathbb{R}^3 and the Lie algebra $su(2)$ of skew-hermitian matrices of trace zero.)

The simplest family of curves arising from system (3) is associated with the plane wave potential $q(x) = a$, at initial time $t = 0$, for the NLS equation; these consist of helices and multiply-covered circles. Setting $k = \sqrt{a^2 + \lambda^2}$, the fundamental solution matrix of (3) for $q(x) = a$ is given by

$$\Psi(x; \lambda) = P \begin{pmatrix} e^{ikx} & 0 \\ 0 & e^{-ikx} \end{pmatrix} P^{-1}, \quad P = \begin{pmatrix} 1 & 1 \\ (i/a)(k - \lambda) & -(i/a)(k + \lambda) \end{pmatrix}. \quad (5)$$

Using the reconstruction formula (4), one computes the components of the position vector of the curve to be

$$\begin{aligned}\gamma_1(x) &= \mathcal{I}m(\Gamma_{11}(x)) = \frac{\sin(2ax)}{2a}, & \gamma_2(x) &= \mathcal{I}m(\Gamma_{12}(x)) = \frac{1}{(2a)} - \frac{\cos(2ax)}{2a}, \\ \gamma_3(x) &= \mathcal{R}e(\Gamma_{12}(x)) = -2\lambda_0 x.\end{aligned}$$

One obtains a closed curve of length L which is an m -times covered circle, $m \in \mathbb{N}$, when a satisfies $aL = 2m\pi$, and the position vector is given by (4) with $\lambda_0 = 0$ (giving γ_3 periodic).

The geometry of these curves is reflected in the associated *Floquet spectrum*. The spectrum $\sigma(q)$ of a given potential $q(x)$ is defined to be the set of all values of the parameter λ for which there exist bounded eigenfunctions of the linear system (3). Since $\det[\Psi(x; \lambda)] = 1$, the spectrum $\sigma(q)$ can be completely characterized in terms of the trace of the transfer matrix $\Psi(L; \lambda)$ across one period L ; this is the *Floquet discriminant*:

$$\Delta(\lambda; q) = \text{Tr}[\Psi(L; \lambda)]. \quad (6)$$

Then $\sigma(q) = \{\lambda \in \mathbb{C} \mid \Delta \in \mathbb{R}, -2 \leq \Delta \leq 2\}$. The fact that the discriminant is an analytic function of λ will be used to investigate the spectrum of perturbations of multiply covered circles. For these solutions, the discriminant is readily computed as

$$\Delta(\lambda; a) = 2 \cos\left(\sqrt{a^2 + \lambda^2 L}\right). \quad (7)$$

It follows that the Floquet spectrum of a multiply covered circle possesses continuous hands given by the union of the real axis and the imaginary interval $(-ia, ia)$, and a discrete set of points at which $\Delta(\lambda; a) = \pm 2$ (see Fig. 1). This *point spectrum* consists of

1. The *simple points* $\lambda = \pm ia$, at which $d\Delta/d\lambda \neq 0$.
2. An infinite number of real double points $\lambda_j = \sqrt{j^2 - m^2}\pi/L$, $j = m + 1, \dots$
3. A total of $m - 1$ *complex double points* $\lambda_n = i\sqrt{m^2 - n^2}\pi/L$, $n = 1, \dots, m - 1$, associated with linear instabilities of the potential.¹
4. A *real point of multiplicity 4*, at $\lambda = 0$, at which the closed curve is reconstructed by means of formula (4).

Note that, since the Floquet spectrum is symmetric under complex conjugation, we need only describe it in the upper half plane.

For finite-gap solutions, it is shown in [6] that, if one reconstructs the curve by means of the Sym–Pohlmeyer formula (4) at a generic real value $\lambda = \lambda_0$, then its position vector is given by

$$\gamma(x; \lambda_0) = \left(\frac{dp(\lambda)}{d\lambda} \Big|_{\lambda=\lambda_0} \right) x + \gamma_0(x; \lambda_0),$$

where $\gamma_0(x; \lambda_0)$ is a quasi-periodic function of x , and $dp(\lambda)/d\lambda$ is the coefficient of the quasi-momentum differential (also known as the Floquet exponent) evaluated at λ_0 . Grinevich and Schmidt [11] derived the closure conditions for the curve associated with a generic periodic finite-gap NLS potential; briefly summarized, these are

¹ One can easily show this by studying the linear stability of $q(x)$ by means of a Fourier expansion.

1. $\lambda_0 \in \mathbb{R}$ must be a real periodic point of the spectrum, i.e. $|\Delta(\lambda_0; q)| = 2$ (corresponding to periodic/antiperiodic eigenfunctions and hence to periodicity of the tangent vector to the curve);
2. λ_0 must be a zero of the quasimomentum differential $dp(\lambda)$.

Since one computes $dp(\lambda)/d\lambda = (d\Delta/d\lambda)/\sqrt{\Delta^2 - 4}$ (see [11]), it follows that $\lambda = \lambda_0$ must be a multiple point of order at least 4 (see [7] for details). In the special case of a multiply covered circle, one sees trivially that the closure condition requires the curve to be reconstructed at $\lambda_0 = 0$, the only real critical point of multiplicity 4 in the associated Floquet spectrum.

3. Perturbing multiply covered circles

In this Section, we set up a perturbation calculation based on the work by Ablowitz et al. [1]. We want to characterize the topology of finite-gap solutions whose spectra are close to the degenerate spectral configuration of a multiply covered circle (the associated NLS potentials are modulationally unstable plane waves), and establish a correspondence between their knot types and their Floquet spectra. In order to do so, one considers perturbed potentials of the form

$$q(x) = a + \epsilon[e^{i\theta_1} \cos(\mu x) + r e^{i\theta_2} \sin(\mu x)] = q_0 + \epsilon q_1, \tag{8}$$

where $0 < \epsilon \ll 1$ and r, θ_1, θ_2 are real parameters; μ is a real frequency to be selected so that the perturbation affects only one specific complex double point. The selection criteria are computed in [1]: for $a = 2m\pi/L$, if $\mu = \mu_j = 2\pi j/L$, $1 \leq \mu \leq m - 1$, then the j th complex double point splits into two simple points and either a gap in the spectrum or a transverse complex band of spectrum appears. The parameters govern the symmetry of the solution: if $\theta_1 = \theta_2 + n\pi$, or if $r = 0$ then the perturbed spectrum exhibits the symmetry $\lambda \rightarrow -\lambda$, and is consequently symmetric about the imaginary axis. (This is due to the potential being an even or odd function of $x - c$; such symmetry is commonly imposed in the study of perturbations of the NLS equation.) On the other hand, if θ_1 and θ_2 are generic, then the perturbation will cause the selected complex double point to split asymmetrically in the complex plane.

Analytic dependence on $q(x) = q_0 + \epsilon q_1$ for the solution matrix of (3) gives an expansion of the form

$$\Phi = \Phi_0 + \epsilon \Phi_1 + \epsilon^2 \Phi_2 + \dots, \tag{9}$$

where $\Phi_0 = P \exp(ik\sigma_3 x)$ is a principal matrix for (3) at $\epsilon = 0$ (compare (5)). We obtain the sequence of inhomogeneous linear systems

$$\frac{d\Phi_k}{dx} - \begin{pmatrix} i\lambda & q_0 \\ -\bar{q}_0 & -i\lambda \end{pmatrix} \Phi_k = Q_1 \Phi_{k-1}, \quad Q_1 = \begin{pmatrix} 0 & q_1 \\ -\bar{q}_1 & 0 \end{pmatrix} \tag{10}$$

for $k \geq 1$, which can be solved recursively using variation of parameters: if $\Phi_k(x) = \Phi_0(x)B_k(x)$ then

$$B_k(x) = \int_0^x \Phi_0^{-1}(t) Q_1(t) \Phi_{k-1}(t) dt. \tag{11}$$

(We normalize $\Phi_k(0) = 0$ for $k \geq 1$.) Using a fundamental matrix $\Psi(x) = \Phi(x)\Phi_0(0)^{-1}$, we compute this expansion for the perturbed Floquet discriminant:

$$\Delta(\lambda; L) = \text{Tr}(\Psi(L)) = 2 \cos(kL) + \epsilon^2 \text{Tr} \left(\Phi_0(L) \int_0^L \Phi_0(t)^{-1} Q_1(t) \Phi_1(t) dt P^{-1} \right) + O(\epsilon^3).$$

The term in ϵ vanishes because q_1 has average value zero. Nonetheless, the analysis in [1] shows that that the spectrum of the perturbed solution—specifically, the location of the periodic points selected by the perturbation differs from the spectrum of the constant potential by $O(\epsilon)$ -terms.

Using the reconstruction formula (4) and the perturbative expansion (9) for the solution matrix of the perturbed system, we can compute the first few terms of the series expansion for the position vector of the corresponding curve. One can verify by direct computation that the curve obtained by truncating the expansion to include the $O(\epsilon)$ -term is a closed curve over the interval $[0, mL]$, and that its associated Floquet spectrum is close to the Floquet spectrum for $q = q_0 + \epsilon q_1$ up to terms of order ϵ^2 or higher. As a consequence, we have the following result (its proof and a more detailed discussion will appear in [6]).

Proposition 3.1. *Given an isoperiodic deformation of the Floquet spectrum of a multiply covered circle, there exists a nearby spectral deformation which is associated to a quasi-periodic potential and which corresponds to a closed curve of periodic curvature and torsion (with $\int_0^{mL} \tau(s) ds \neq 0$ in general).*

So, by relaxing the requirement that the perturbed potential be periodic, we can achieve the closure condition for the associated curve (whose Floquet spectrum will thus contain a real multiple point of multiplicity 4 or higher).

4. Experiments

In this Section, we show several interesting cases of closed curves obtained by truncating the perturbation expansion (9) at order ϵ and using the Sym–Pohlmeyer reconstruction formula (4). We discuss the relation between their knot types and the Floquet spectrum of the corresponding NLS potentials, shown next to each curve plot.

4.1. The even case

If $\theta_1 = \theta_2$ or $\theta_1 = \theta_2 + \pi$ or $r = 0$, the perturbed potential is an even or odd function of $x - c$, and the complex double points affected by the perturbation form cross or gap configurations invariant under reflection in the imaginary axis. When the perturbation selects only one complex double point, the corresponding curves are self-intersecting. The second author has shown, using the Baker function representation, that this is the case for curves associated to any modulated two-phase NLS potentials with symmetric spectrum; details will appear in [6].

4.2. The noneven case

For generic values of θ_1 and θ_2 the corresponding curves are not self-intersecting, and interesting knot types arise. The first four figures show the knots arising when a single complex double point is split at order ϵ by the perturbation. All the experiments done in this case produce (m, j) -torus knots; m is the number of strands the knot wraps around the axis of revolution of the torus, and j the number of strands wrapped around the waist of the torus. The integers m and j are related to the complex part of the discrete spectrum of the associated NLS potential: $m - 1$ is the number of complex double points in the spectrum of the unperturbed solution, and j is the location of the complex double point which splits under the perturbation ($j = 1$ marks the double point closest to the upper end of the imaginary band).

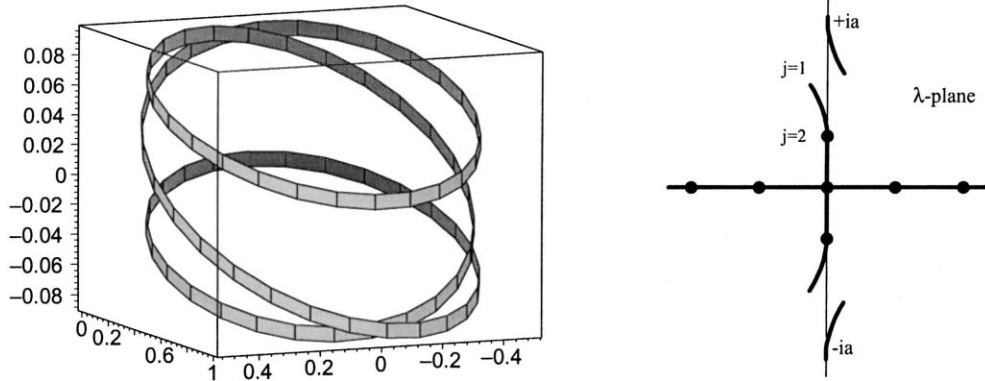


Fig. 2. An unknot [a (3, 1)-torus knot] with $m = 3$, $j = 1$, $\epsilon = 0.1$, $r = 0.2$, $\theta_1 = \pi/2$, $\theta_2 = 0$.

In Fig. 2, we show a (3, 1)-torus knot and the corresponding Floquet spectrum. In this case, we have perturbed a triply-covered circle (or a plane wave potential with three unstable modes), and the perturbation resonates with the first of the unstable modes $\exp(2\pi i/L)$.

Figs. 3 and 4 show two trefoil knots ((3, 2)-torus knots) of opposite handedness. A right-handed trefoil has positive crossings.

In each of the two cases, the perturbation resonates with the second unstable mode $\exp(4\pi i/L)$, and causes the top part of the imaginary band to move within the first or second quadrant of the complex plane depending on the values of the θ_i 's. In [1], it is observed that the two asymmetric spectral configurations are associated with initial conditions for modulated right and left traveling wave solutions. The handedness of the knot is thus related to the sign of the velocity of such potentials.

In Fig. 5, we show another example of a left-handed (5, 2)-torus knot coming from a perturbed plane wave potential with four unstable modes. The second complex double point has split asymmetrically, with the end of the top imaginary band moving into the left-half plane.

When the perturbation causes one of the complex double points to split asymmetrically, we can formulate a precise conjecture about the relation between Floquet spectra and knot types.

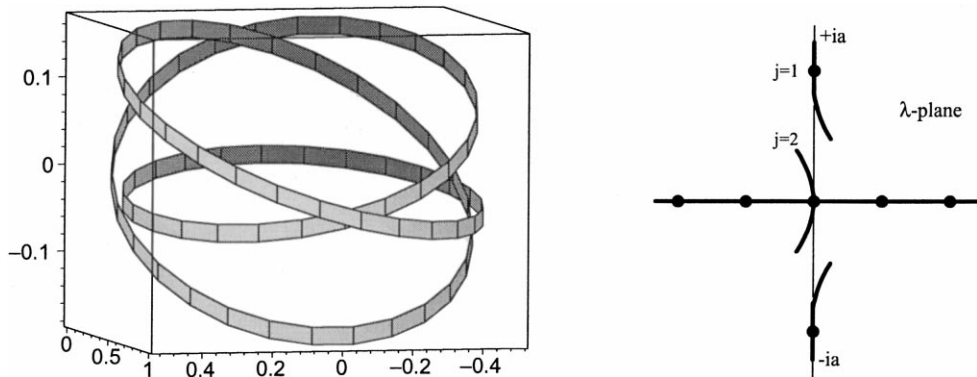


Fig. 3. A left-handed trefoil and its spectrum: $m = 3$, $j = 2$, $\epsilon = 0.1$, $r = 0.2$, $\theta_1 = \pi/2$, $\theta_2 = 0$.

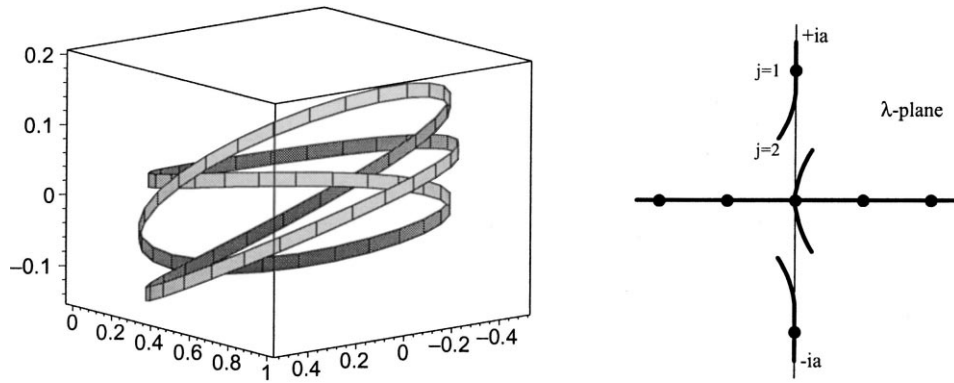


Fig. 4. A right-handed trefoil and its spectrum: $m = 3$, $j = 2$, $\epsilon = 0.1$, $r = 0.2$, $\theta_1 = -\pi/2$, $\theta_2 = 0$.

Conjecture 4.1. *A noneven perturbation of a plane wave solution with m unstable modes which causes the j th complex double point alone to split at first order corresponds to an (m, j) -torus knot, whose handedness is labeled in terms of the right/left splitting of the complex band of spectrum.*

In terms of homoclinic orbits of multiply covered circles, this would imply that the self-intersecting curve generated by a single Bäcklund transformation of an m -covered circle performed at the j th complex double point separates two (m, j) -torus knots of opposite handedness.

Finally, we have evidence that two noneven perturbations which individually select different complex double points may be superimposed to generate knot types that go beyond torus knots. More explicitly, we set

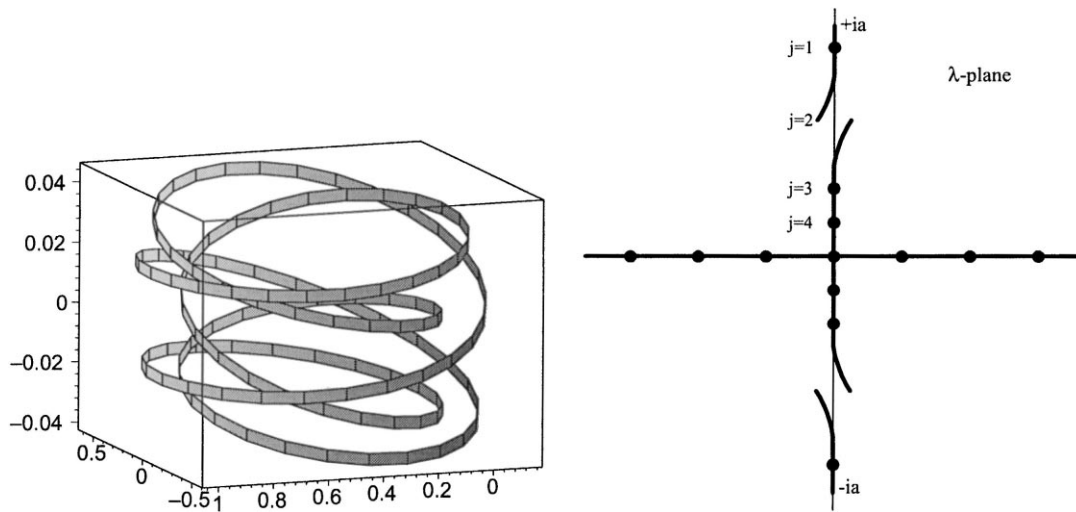


Fig. 5. A left-handed $(5, 2)$ -torus knot: $m = 5$, $j = 2$, $\epsilon = 0.1$, $r = 1$, $\theta_1 = 0$, $\theta_2 = \pi/6$, and the Floquet spectrum of the corresponding NLS potential (the initial condition for a modulated left-traveling wave).

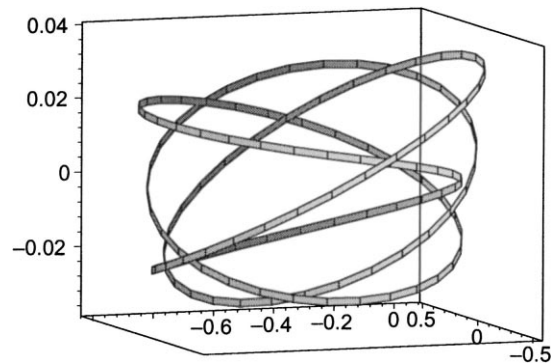


Fig. 6. Knot produced with $m = 4$, $j = 3$, $k = 2$, $\theta_1 = 0$, $\theta_2 = \pi/6$, $\theta_3 = 0$, $\theta_4 = \pi/2$, $r = 1$, $s = 4$, $t = 1$ and $\epsilon = 0.01$. The knot type (labeled 5_2 in standard knot tables) has minimum crossing number 5 and is not a torus knot.

$$q(x) = a + \epsilon [e^{i\theta_1} \cos(\mu_j x) + s e^{i\theta_2} \sin(\mu_j x) + r(e^{i\theta_3} \cos(\mu_k x) + t e^{i\theta_4} \sin(\mu_k x))],$$

where r, s, t are real, and $j \neq k$ are integers between 1 and $m - 1$ selecting the double points to be perturbed. Experiments (see Fig. 6) suggest that, in order to generate new knot types, j and k should be relatively prime, with at least one of them relatively prime to m , and that genuinely noneven perturbations — with generic values for all parameters—must be used.

Acknowledgements

The first author is partially supported by NSF grant DMS-9705005. All figures were produced using Maple V.

References

- [1] M.J. Ablowitz, B.M. Herbst, C.M. Schober, Computational chaos in the nonlinear Schrödinger equation without homoclinic crossings, *Physica A* 228 (1996) 212–235.
- [2] E.D. Belokolos, A.I. Bohenko, V.Z. Enol'skii, A.R. Its, V.B. Matveev, *Algebro-Geometric Approach to Nonlinear Integrable Equations*, Springer, New York, 1994.
- [3] A. Calini, A note on a Bäcklund transformation for the continuous Heisenberg model, *Phys. Lett. A* 203 (1995) 333–344.
- [4] A. Calini, T. Ivey, Bäcklund transformations and knots of constant torsion, *J. Knot Theory Ramif.* 7 (1998) 719–746.
- [5] A. Calini, T. Ivey, Topology and Sine-Gordon evolution of constant torsion curves, *Phys. Lett. A* 254 (1999) 170–178.
- [6] A. Calini, T. Ivey, Finite-genus solutions of the vortex filament equation, in press.
- [7] A. Calini, T. Ivey, Connecting geometry, topology and spectra for finite-gap NLS potentials, in preparation.
- [8] A. Doliwa, P.M. Santini, An elementary geometric characterization of the integrable motion of a curve, *Phys. Lett. A* 185 (1994) 373–384.
- [9] Y. Fukumoto, R.L. Ricca, *Vortex Filament Motion and Related Integrable Systems*, World Scientific, Singapore, 1999.
- [10] R. Goldstein, D. Petrich, Solitons, Euler's equations, and vortex patch dynamics, *Phys. Rev. Lett.* 69 (1992) 555–558.
- [11] P.G. Grinevich, M.U. Schmidt, Closed curves in R^3 : a characterization in terms of curvature and torsion, the Hasimoto map and periodic solutions of the filament equation, *dg-ga/9703020* (1987) (preprint).
- [12] H. Hasimoto, A soliton on a vortex filament, *J. Fluid Mech.* 51 (1972) 477–485.
- [13] G.L. Lamb, *Elements of Soliton Theory*, Wiley/Interscience, New York, 1980.

- [14] J. Langer, R. Perline, Geometric realizations of the Fordy–Kulish nonlinear Schrödinger systems, *Pacific J. Math.* (2000), in press.
- [15] K. Pohlmeyer, Integrable Hamiltonian systems and interactions through quadratic constraints, *Commun. Math. Phys.* 46 (1976) 207.
- [16] R.L. Ricca, Torus knots and polynomial invariants for a class of soliton equations, *Chaos* 3 (1913) 83–91.
- [17] A. Sym, Soliton surfaces and their applications in: geometrical aspects of the Einstein equations and integrable systems, *Lecture Notes Phys.* 239 (1985) 154.
- [18] C. Wexler, A.T. Dorsey, Solitons on the edge of a two-dimensional electron system, *Phys. Rev. Lett.* 82 (1999) 620–623.